Is sugar metabolism in cambial region able to explain the tolerance to water deficit in poplar?

Running title: Sugar metabolism regulates poplar tolerance to water deficit

Silvia Traversari[a], Alessandra Francini[a], Maria Laura Traversi[b], Giovanni Emiliani[b], Carlo Sorce[c], Luca Sebastiani[a*], Alessio Giovannelli[a,b]

[a]Institute of Life Sciences, Scuola Superiore Sant'Anna, Piazza Martiri della Libertà, 33, 56127, Pisa, Italy
[b]Trees and Timber Institute (IVALSA-CNR), Via Madonna del Piano, 10, 50019, Sesto F.no (Florence), Italy
[c]Department of Biology, University of Pisa, Via Luca Ghini, 13, 56126, Pisa, Italy

Silvia Traversari, s.traversari@santannapisa.it
Alessandra Francini, a.francini@santannapisa.it
Maria Laura Traversi, traversi@ ivalsa.cnr.it
Giovanni Emiliani, giovanni.emiliani@gmail.com
Carlo Sorce, carlo.sorce@unipi.it
Luca Sebastiani, *corresponding author, l.sebastiani@santannapisa.it; tel: + 39 050 883070
Alessio Giovannelli, giovannelli@ivalsa.cnr.it

Date of re-submission: 09/04/2018
Number of tables: 2 + 2 in supplementary data
Number of figures: 8 + 5 in supplementary data
Word count: 5474

HIGHLIGHT

In two poplar species with contrasting growth performance, sugar metabolisms in xylem and cambial region are able to explain the different grades of tolerance to drought and the recovery rates after water deficit.

ABSTRACT

Drought dramatically affects wood production by adversely impacting cambial cells and their derivatives. Both photosynthesis and assimilate transport are consequently affected by drought. Two poplar genotypes *Populus deltoides* 'Dvina' and *Populus alba* 'Marte' had contrasting growth performances and water-carbon balance strategies; a mechanistic understanding of water-deficit response was provided by these poplar species. It was found demonstrated that 'Marte' was more anisohydric than 'Dvina'. This behaviour was associated with the capacity to reallocate carbohydrates during water deficit. In contrast, 'Dvina' displayed a more conservative water management; carbohydrates were preferably stored or used for cellulose production rather than being used to achieve an osmotic balance between phloem and xylem. Data confirmed that the more 'risk-taking' behaviour of 'Marte' allowed a fast recovery after water deficit and it was connected with a different carbohydrate metabolism.

KEY-WORDS

cambial region; carbohydrates; carbon turnover; Populus; recovery; starch; water deficit.

INTRODUCTION

Drought dramatically affects the production and yield of plants worldwide. It is expected to occur more often under on-going global climatic changes (Shao *et al.*, 2008; Osakabe *et al.*, 2014). Water deficit impairs wood formation directly by decreasing turgor pressure in cambial cells and their derivatives (Shao *et al.*, 2008; Korner, 2015). Moreover, following the reduction of photosynthesis and assimilate transport, carbon is depleted in cambial region (Diaz-Espejo and Hernandez-Santana, 2017). Hydraulic failure, carbon starvation and phloem failure are principal processes that occur in woody plants under water deficit. All of them translate into a decrease in plant growth and an increase in tree mortality (Anderegg *et al.*, 2012). The relationship between transport failure and carbon sink depletion is being investigated currently (Hartmann, 2015), but some evidence shows that drought tolerance strategies may be based on the modulation of carbohydrate metabolism and osmotic balance (Sevanto *et al.*, 2014). There is a strong relationship between phloem and xylem tissues that ensure a balance between carbon and water (Diaz-Espejo and Hernandez-Santana, 2017). Thus, the relationship between transport failure and carbon sink depletion has to be studied carefully by considering the possible integration and coordination of phloem and xylem tissues.

Cambial region includes cambium, which is composed of meristematic cells called as "initials", and mother cells of xylem and phloem that undergo expansion and differentiation processes (Uggla and Sundberg, 2002). The rate and duration of cambium activity and cell differentiation determine xylem traits, which are crucial for defining the efficiency of water and nutrient transport from roots to shoots (Sorce *et al.*, 2013) as well the mechanical properties of wood (Lachenbruch and McCulloh, 2014). In this context, useful information can be obtained by studying metabolic processes that occur in cambial region during water deficit.

Poplar species can provide a mechanistic understanding of water deficit responses in trees. Within *Populus* genus, different species show contrasting water-use efficiencies and adaptive strategies under drought (Yin *et al.*, 2004, 2005; Monclus *et al.*, 2009). In poplar species, the sensitivity of cambial region to water deficit was a genotype-dependent feature; it was related to the activation of different metabolic pathways and opposite osmotic regulation strategies (Pallara *et al*., 2012). Water deficit in *Populus deltoides* 'Dvina' affected anatomical properties of xylem, which was produced after rehydration (Cocozza *et al.*, 2011). In contrast, xylem features of *Populus alba* 'Marte' were unchanged (Luisi *et al.*, 2014). The ability to restore cambium cell division is a key point, which allows fast recovery after rehydration. The crucial checkpoint for mitosis is regulated by B-type cyclins (Fowler *et al*., 1998) and in poplar species gene transcriptions of isoforms *CycB1.3-4* and *CycB2.1* were highest in dedifferentiated tissues (Emiliani *et al*., 2016). We hypothesized the role of these genes in the genotype-dependent response of cambial region to water deficit. Moreover, the

analysis of B-type cyclins in cambial region was combined with the analysis of stem radial variations through point dendrometers. This allowed to verify the hypothesis proposed by Zweifel *et al.* (2016) that stem growth breaks off during tree water deficit (Zero Growth, ZG-concept).

Many studies have reported about the involvement of soluble sugars in response to water deficit (Galvez *et al.*, 2011; Adams *et al*., 2013; Sengupta and Majumdar, 2014; Sevanto *et al.*, 2014; Spicer, 2014; Zwieniecki and Secchi, 2015). Carbohydrates stabilise proteins and membranes, provide osmotic adjustments and energy reserves for recovery after rehydration. Furthermore, these molecules operate as signal molecules, eliciting growth and stress responses (Santos and Pimentel, 2009, Emiliani *et al.*, 2016). Water deficit activates osmotic adjustments by fluctuating non-structural carbon compounds (Blum, 2017), which are in stored and non-stored formats. Although sucrose/starch pathway was usually studied by only considering the amount of carbohydrates (Sala *et al*., 2012; Adams *et al*., 2013; Lintunen *et al*., 2016), different genotype-dependent responses could be explained by analysing some candidate genes associated with sucrose/starch conversion. The degradation of sucrose was monitored by gene transcription of *Sus2* and *Sus3* sucrose synthases, the two isoforms predominantly expressed in cambial region of poplar species (Zhang *et al*., 2011). The interest on *Sus2* gene was due to its involvement in biosynthetic pathway of cellulose (Konishi *et al*., 2004; Coleman *et al*., 2009) to assess a possible investment in cellulose production as previously suggested in *P. deltoides* during water deficit (Cocozza *et al*., 2011). The synthesis and degradation of starch was monitored by gene transcription of starch synthases (*SS*) and α- and β-amylases (*Amy* and *Bam*). It was found that starch synthases elicited drought response in poplar species (Street *et al*., 2006) and *SS2* and *SS4* in *Arabidopsis thaliana* seemed to be involved in different functions, such as starch chain elongation and starch granule initiation, respectively (Streb and Zeeman, 2012). In poplar species, osmotic stress induced the expression of α-amylase genes, such as *Amy1.1-2* (Bae *et al*., 2010). By other hand, β-amylase genes, as *Bam5*, were involved in the refilling of embolized vessels (Secchi and Zwieniecki, 2011). Moreover, *Bam5* was transcriptionally induced by sugars and it was the only β-amylase with cytosolic localization (Monroe *et al*., 2014). At least, the carbohydrate transport could be investigated by the gene transcription of sucrose transporters, such as *Suc2.1*, *Sut2.a-b*, and *SUT4*, for their role in drought response in poplar xylem (Secchi and Zwieniecki, 2011).

Within this context, we performed an experiment to validate mechanistic hypothesis that genotype-dependent tolerance to water deficit could be explained by regulating specific metabolic pathways related to sugar metabolism in cambial region of poplar species. In particular, our hypotheses were as follows: (1) poplar species showing fast recovery after water deficit exhibit greatest plasticity in sucrose/starch pathway; (2) the carbohydrate metabolism of cambial region is associated with

different genotypic responses under water deficit; and (3) genes related to cell cycle and sucrose/starch pathway elucidate different degrees of poplar tolerance to water deficit.

MATERIALS AND METHODS

Plant material and treatment

One-year old plants of *Populus deltoides* Marsch 'Dvina' and *Populus alba* L. 'Marte' clones were grown in pots with a combination of peat/sand/perlite (50/40/10 v/v/v, pH = 6.8) at a nursery of CNR-IVALSA in Florence (43°49'06"N 11°12'08"E), as described by Luisi *et al.* (2014). For each genotype, twenty plants were selected for dimensional uniformity. On 12th July (t_0), three plants of each genotype were sampled and remaining plants were subjected to different watering regimes (n = 4) during 21 d of treatment. Soil moisture was kept at field capacity (water content was 30% w/w of total soil weight) in well-watered plants (WW). Watering was suspended for 8 d (t_{max}) and then resumed up until 13 d (t_{rec}) in water limited plants (WL). Figure 1 illustrates experimental plan. During the experiment, meteorological data were recorded by LAMMA – Laboratory of Monitoring and Environmental Modelling for Sustainable Development, Florence (http://www.lamma.rete.toscana.it/eng/index.html – weather station was located at experimental site).

Soil–Plant Water Relations

Substrate volumetric water content was measured every day in WW and WL plants by Hydro-sense probes (Campbell Scientific Inc., Logan, USA), which were based on time-domain reflectometry. The relative extractable water in the substrate (REW) was calculated as follows:

$REW = (SWC_a - SWC_{wp}) / (SWC_{fc} - SWC_{wp})$ (Eqn 1)

Here SWC_a is the water content of actual substrate in root zone; SWC_{wp} is the water content of substrate at wilting point (9% w/w); SWC_{fc} is the water content of substrate at field capacity (30% w/w).

Leaf analyses

Leaf water potential of predawn and midday (Ψw_{pd} and Ψw_{md}, MPa) was determined from two fully expanded leaves of each plant (leaf plastochrone index was between 5 and 7) with the help of pressure chamber (PMS Instruments Co., Corvallis, OR, USA). Leaf water content (LWC) was determined from three fully expanded leaves, which were excised before dawn (LWC_{pd}) and at midday (LWC_{md}). Fresh leaves were excised and weighed (FW). Then, they were dried at 80 °C for 48 h, and dry weight (DW) was determined.

We used the following equation to calculate LWC:

LWC = 100 *x* (FW - DW) / DW (Eqn 2)

The difference between predawn and midday ($\Delta LWC_{pd\text{-}md}$) was also calculated.

Leaf stomatal conductance (g_s, mol m^{-2} s^{-1}), transpiration rate (E, mmol H_2O m^{-2} s^{-1}) and net CO_2 assimilation rate (A_{max}, µmol CO_2 m^{-2} s^{-1}) were measured on intact fully expanded leaves (leaf plastochrone index was 6 or 7) between 1 p.m. and 2 p.m. with the help of a portable open system (ADC-LCA3, Analytical Development, Hoddesdon, UK). This system operated at a flow rate of 5.7 ml s^{-1} and an ambient CO_2 pressure of 33±1 Pa. Photosynthetic flux density was greater than 1200 µmol m^{-2} s^{-1}. Instantaneous water use efficiency (WUE*i*, mmol CO_2 mol H_2O^{-1}) was determined as instantaneous leaf transpiration efficiency, A_{max}/E. Specific leaf area (SLA, m^2 kg^{-1}) was calculated at t_{max}.

Stem analyses

The variations in stem radius were monitored with automatic point dendrometers, which were constructed for small stems. Dendrometers consisted of a linear variable transducer (RS Pro LM10 Series, Rs Component s.r.l., Italy), which was used to measure linear displacement of a stainless steel sensing rod (effective travel = 10 mm ± 0.5 mm, linear thermal expansion coefficient = 2.5 × 10^{-6} K^{-1}). This rod was pressed against the bark. Transducer was mounted on a polytetrafluoroethylene frame fixed with three titanium rods to the stem, which was 10–15 cm above the ground. The frame was anchored to a polytetrafluoroethylene holder fixed on two sides of the pot. As the stem expands or contracts, the rod transmits the signal to the transducer. Sensor output V_1/V_x ratio was converted into value (length of sensor, mm) by using a linear calibration regression equation (Loggernet software, Campbell Scientific Inc., Logan, USA). A total of sixteen plants (four plants for each genotype and treatment) were monitored with dendrometers, which were installed at 1/4 height from the collar. Aluminium foil was used to shield all the dendrometers from direct sunlight and weather damage. Raw data were recorded every 15 min, and averages were calculated at each hour.

Growth-induced irreversible stem expansion (GRO) and tree water deficit-induced reversible stem shrinkage (TWD) were determined by following the procedure reported by Zweifel *et al.* (2016); it was assumed that growth could only take place in the absence of stem radius shrinkage (ZG-concept). Moreover, TWD (µm) was defined as the difference between the previous maximum stem radius (SR_{max}) and current stem radius (SR_t) when $SR_t < SR_{max}$. Furthermore, GRO (µm) was calculated as the difference between SR_t and highest previous value of SR_{max} when $SR_t > SR_{max}$.

The rates of stem growth over time ($\Delta SR/\Delta_t$, µm h^{-1}) were calculated as follows:

$\Delta SR/\Delta_t$ = (GRO - TWD) / Δ_t (Eqn 3)

Instantaneous stem water deficit, ΔW (μm), was extracted by de-trending original growth data of dendrometers with the help of piecewise linear regression (Supplementary Fig. S1).

At each sampling time, stem portions (50 mm) were excised 20 cm from the collar. Pith was discarded after separating the bark immediately from xylem. Samples were weighed within 5 min after harvest for determining fresh mass (M_f) and then fresh volume (V_f) by water displacement (Haworth *et al.*, 2017). Dry mass (M_d) was determined after 96 h at 103 °C. Relative water content (RWC, %) was determined for bark and xylem by using the following formula:

$RWC = (M_f - M_d) / (V_f - V_d) \times 100$ (Eqn 4)

Here dry volume (V_d) was estimated by dividing M_d with 1.53; density value was assumed for dry cell wall material (Pallara *et al.*, 2012).

Wood moisture content (α) was determined according to Berry *et al.* (2005) at each sampling time. Basic wood density was defined as the ratio between dry mass and saturated volume (Rosner, 2017). Briefly, stem discs of 8–10 mm were collected and two prismatic sub-samples of xylem were taken by excluding pith and bark. Samples were weighed immediately, and dry mass was calculated after 96 h at 103 °C. To record saturated volume, fresh woody samples were immersed in distilled and degassed water under partial vacuum (10 KPa) for 72 h.

Roderick *et al.* (2001) proposed the following formula to calculate fibre saturation point (α_f):

$$\alpha_f = \frac{0.22}{\sqrt{\frac{basic\ density}{\rho_w}}} \text{ (Eqn 5)}$$

Here ρ_w is the density of liquid water (kg m^{-3}).

The difference α-α_f is the amount of free water available to support hydraulic network.

Cambial region and mature xylem sampling

Stems were divided into logs of 10–15 cm; these logs were frozen immediately in liquid nitrogen. Then, they were subjected to freeze-drying under vacuum. To obtain samples from cambial region, bark was detached from logs and differentiating phloem and xylem were softly scraped from inner side of bark and outermost side of xylem. Xylem was converted into a fine powder with the help of Ultra Centrifugal mill ZM 200 (Retsch, Haan, Germany). The complete procedure was reported in Giovannelli *et al.* (2011).

Soluble carbohydrate and starch quantification

According to a procedure reported by Giovannelli *et al.* (2011), soluble carbohydrate and starch analyses were performed on cambial region and xylem; the extraction was modified by using water

(Milli Q grade, pH = 7) as the extraction solvent. Briefly, sugar content was determined by high performance liquid chromatography equipped with a SHODEX SUGAR Series SC 1011 8 × 300 mm column (Showa Denko, Germany), which was preceded by a pre-column Guard Pak Insert Sugar Pak II (Waters). Water (Milli Q grade) was used as the mobile phase, with a flow rate of 0.5 mL min^{-1}. Soluble sugars were identified with a refractive-index detector (LC-30 RI, Perkin Elmer); carbohydrate standards were used for corroboration of identified sugars (Sigma-Aldrich, St. Louis, MO, USA). Finally, sorbitol was used for normalizing sugar amounts (Harris, 1997). After extracting soluble sugars, starch was analysed in remaining powder.

The contribution to the osmotic potential of sucrose, glucose and fructose was determined by following formula (Gucci *et al*., 1997):

$\Psi\pi_{sat}$ (sucrose/fructose/glucose) = RT × (RDW) × C (Eqn 6)

Here $\Psi\pi_{sat}$ indicates the contribution (MPa) of individual sugars to $\Psi\pi$; RDW is the relative dry weight at saturation (kg m^{-3}); C is the molar concentration of solutes (mol kg^{-1}); and RT value at 25 °C is -0.002479 m^3 MPa^{-1} mol^{-1}.

Determination of osmotically active molecules

At each sampling time, osmotically active solutes were determined by following the procedure described in a study conducted by Arend and Fromm (2007). Dried powders (4 mg) of cambial region and xylem were suspended in 250 μL of distilled water. Samples were vortexed and sonicated for 10 min. Then, they were centrifuged at 10000 *g* for 5 min, and supernatants were analysed by a freezing point osmometer (Osmomat 030 Gonotec, Germany). Results were expressed in mosm g^{-1} DW.

Histological observations

At each sampling time, stem disks of 10–20 mm thickness were cut at 30 cm from the collar. Then, they were placed in ethanol (95%) and stored at 4 °C. Then, disk sections were fixed with ice on a Peltier plate. Finally, these sections were cut into transverse or radial sections of 8–12 μm thickness with a rotary microtome Leica RM2245. The sections were stained with Lugol's solution (Sigma-Aldrich, St. Louis, MO, USA). These sections were observed with Nikon Eclipse 800E light microscope (Melville, NY, USA).

Primer design

We evaluated mRNA transcriptions of following genes: B-type Cyclin *CycB1.3-4* and *CycB2.1*, amylase *Amy1.1-2* and *Bam5*, starch synthase *SS2* and *SS4*, sucrose synthase *Sus2* and *Sus3*, and

sugar transporter *Suc2.1*, *Sut2.a-b* and *SUT4*. Primers for housekeeping genes *Act-2* and *Ef-1* were gained according to Brunner *et al.* (2004) and Pallara *et al.* (2012), respectively. Primers for *CycB1.3-4 and CycB2.1* genes were obtained from Emiliani *et al.* (2016). New primers were designed for other genes. To enable primer design, nucleotide sequences of *P. trichocarpa* genes were retrieved from Popgenie database (www.popgenie.org – Sjödin *et al.*, 2009) with BLAST search tool. Sequences of homologue genes of *A. thaliana*, were retrieved in TAIR database (www.arabidopsis.org – Huala *et al.*, 2001). Sequences showing significant hits were aligned with Muscle (Edgar, 2004) and trimmed to eliminate poorly aligned regions. A Neighbour Joining tree (1000 bootstrap) was built with Mega 6 program (Tamura *et al.*, 2011). To construct dendrogram for *sucrose synthase* genes, sequences and isoforms nomenclature was reported in a study conducted by Zhang *et al.* (2011). For the identification of *sucrose transporter* genes, was used the same nomenclature adopted by Secchi and Zwieniecki (2011). Principal features of primers used are reported in Supplementary Table S1.

RNA isolation and RT-PCR analysis

According to a procedure described by Chang *et al.* (1993), total RNA was extracted from cambial region powder in three biological replicates for each treatment and time. The extraction methodology was adjusted by replacing spermidine with β-mercaptoethanol in extraction buffer. The quality of RNA was verified by performing agarose gel electrophoresis. Then, RNA was quantified with NanoDrop 2000 spectrophotometer (Thermo Fisher Scientific, Waltham, MA, USA). To eliminate DNA contamination, 3 μg of total RNA was treated with *DNAse* by using the "*DNAse* I Amplification Grade" kit (Invitrogen, Thermo Fisher Scientific, Waltham, MA, USA) according to manufacturer's procedure. After treatment with *DNAse*, RNA was precipitated with LiCl and re-suspended in 50 μL of DEPC water. Using reverse-transcription polymerase chain reaction method, RNA was retro-transcribed in first-strand complementary DNA (cDNA) with "SuperScript VILO^{TM} MasterMix" (Invitrogen, Thermo Fisher Scientific, Waltham, MA, USA) according to manufacturer's procedure. Reaction was performed with random primers in 25 μL of final volume. To determine the accumulation of target gene mRNA, cDNA was used in RT-PCR (details of primer design are presented below in this paper). By using the ΔΔCq method (Pfaffl, 2001), the results were compared with the reference genes *Act-2* and *Ef-1*. Target and reference gene-specific amplification efficiencies were calculated from quantification cycles (Cqs) of all cDNA samples. For each gene and poplar genotype, a 5-point dilution set of two standard samples was amplified in duplicate reactions and reaction efficiency was verified. Then, RT-PCRs were carried out in duplicate reactions for each sample; outcomes were discarded if the difference in Cq

numbers was higher than 0.5 for replicates. For each gene, a no template control was amplified in each run. For all primers, RT-PCRs were conducted with an annealing temperature of 60 °C by using the "iTaq™ Universal SYBR® Green Supermix" kit (Bio-Rad, California, USA). In a final volume of 10 µL, the reaction was performed with 10 µM of each primer and 1 µL of 1:5 dilution of template cDNA. The RT-PCR protocol was as follows: 95 °C for 5 s and 60 °C for 30 s; a total of 40 amplification cycles were performed. At the end of amplification cycles, the melting curve was calculated for each amplification.

Statistical analysis

All analyses were performed on four biological replicates (n = 4). Then, RT-PCR analysis was performed on three biological replicates (n = 3). Data were checked for normal distribution (D'Agostino-Pearson K^2 test). The effect of water regime and genotype was assessed with two-way analysis of variance (ANOVA). *Post hoc* analysis was conducted with LSD Fisher test. Furthermore, *t*-test analysis was performed at t_0 sampling time (n = 3). Data that did not have a normal distribution and percentages were transformed before ANOVA. Correlation was evaluated by performing Pearson test. All analyses were executed with NCSS Data Analysis software. All graphs were plotted with Prism 5 software (GraphPad, La Jolla, CA, USA).

RESULTS

Physiological and biochemical comparison between poplar genotypes in well-watered conditions

Under WW conditions, the two genotypes 'Dvina' and 'Marte' displayed different morpho-physiological and biochemical traits that highlighted contrasting growth performances and water-carbon balance strategies. The genotype 'Marte' showed a higher growth than the genotype 'Dvina', both in terms of stem growth rate ($\Delta SR/\Delta_t$, Fig. 2A) and stem elongation (1.6 *vs* 1.0 mm d^{-1}, data not shown). Compared to 'Dvina', 'Marte' had higher RWC in bark (Fig. 3A, 92 *vs* 88%, respectively) and a lower instantaneous stem water deficit (ΔW, Fig. 2B). In contrast, RWC and basic density (366.6 in 'Divina' *vs* 306.5 kg m^{-3} in 'Marte', $P = 0.003$) of xylem were significantly higher in 'Dvina' than in 'Marte' (Fig. 3B). But free water available to support hydraulic network (α-α_f) was not significantly different for two genotypes (Table 2).

Under WW condition, leaves of 'Marte' displayed higher specific leaf area and $\Delta LWC_{pd\text{-}md}$ than 'Dvina'; however, this difference did not induce significant changes in leaf $\Delta\Psi w_{pd\text{-}md}$ and WUE*i* between genotypes (Table 2). Genotypes displayed different carbohydrate concentration within cambial region and xylem (Table 1). 'Dvina' had significantly more starch than 'Marte' within

xylem, and this accumulation was even higher in cambial region. The highest concentration of starch was corroborated by histological observation with Lugol's solution (Supplementary Fig. S2A-C). In contrast, 'Marte' contained higher concentration of soluble sugars, mostly glucose, in cambial region. Thus, 'Marte' had a higher total $\Psi\pi_{sat}$ than 'Dvina' (Table 1 and Supplementary Table S2).

Physiological and biochemical comparison between poplar genotypes in water limited conditions and after rehydration

The intensity of water deficit was determined from relative extractable water of substrate (Fig. 4). The results indicate that both genotypes were subjected to same water deficit intensity and duration, which was in the range of 0.05 and 0.40 (genotype effect, $0.060 \leq P \leq 0.617$). However, after 8 d of suspension of irrigation (t_{max}), some traits were affected to different extents depending on genotype. Stem elongation (data not shown) was negatively affected in 'Dvina' ($P = 0.004$), but not in 'Marte' ($P = 0.220$). In contrast, $\Delta SR/\Delta_t$ (Fig. 2A) was zero in 'Marte' WL plants, while a reduction of 91% was detected in 'Dvina' WL *vs* WW plants.

On the whole, 'Marte' showed more variations in physiological and biochemical parameters. In 'Marte', a significant reduction of $\Delta LWC_{pd\text{-}md}$ (-37%) was recorded in WL plants as compared to WW plants; however, no significant differences were observed in 'Dvina' plants. With this conservative strategy, 'Dvina' WL plants maintained a significantly higher leaf $\Delta\Psi w_{pd\text{-}md}$ than 'Marte' (0.5 *vs* 0.1 MPa, respectively). Both genotypes showed a decrease in RWCs of bark and xylem (Fig. 3), which matched with an increase in instantaneous stem water deficit (ΔW, Fig. 2B) and a decrease in $\alpha\text{-}\alpha_f$ (Table 2). In 'Marte' WL plants, statistically higher decrease of $\alpha\text{-}\alpha_f$ was associated with a low level of free water that was available to support hydraulic network at t_{max}.

Water deficit induced contrasting effects on genotype of soluble sugar and starch contents within xylem and cambial region (Table 1 and Supplementary Table S2). Starch content decreased while sucrose content increased significantly in the xylem of 'Marte' WL plants. These modifications were associated with a significant increase in sucrose $\Psi\pi_{sat}$ and a higher sucrose/starch ratio ($P < 0.05$ – *t*-test between WW and WL plants). In contrast, sucrose content decreased significantly in cambial region of 'Marte' ($P < 0.05$ – *t*-test between WW and WL plants). Compared to WW plants, no variations were observed in soluble sugars and starch of 'Dvina' WL plants.

After 13 d from resumption of irrigation (t_{rec}), both genotypes showed complete restoration of primary and secondary growth, $\Delta SR/\Delta_t$, ΔW, bark RWC, (Fig. 2, Fig 3A), $\Delta LWC_{pd\text{-}md}$, leaf $\Delta\Psi w$, and WUE*i* (data not shown). The only exception was xylem RWC (Fig. 3B), which was lower in WL plants than in WW plants. Thus, water content was incompletely restored in this compartment

($P < 0.05$ – *t*-test between WW and WL plants for both genotypes). With regards to carbohydrates (Table 1 and Supplementary Table S2), sucrose increased in 'Dvina' cambial region (+15% on average) but decreased in 'Marte.' During the experiment, starch concentration increased in parenchyma cells of xylem tissue in both genotypes and treatments. This was corroborated by histological observations (Supplementary Fig. S2B-D).

During the experiment, soluble sugars and osmotically active molecules showed a significant correlation in the xylem of 'Marte,' ($R = 0.837$, $P < 0.001$; Supplementary Fig. S3) which was not observed in 'Dvina'.

Gene transcription

The mRNA accumulations of target genes showed genotype and treatment dependent responses. Cyclin B genes, specifically *CycB1.3-4* and *CycB2.1* isoforms (Fig. 5A-B, respectively), showed a very strong decrease of transcription at t_{max} in WL plants. Moreover, *CycB1.3-4* gene basal level of transcription was not restored at t_{rec} in 'Dvina' WL plants (Fig. 5B). Two-way ANOVA indicated that B1 type Cyclin was more influenced by genotype and water regime than B2 type Cyclin.

Except for *Sus2* and *Bam5* genes, sucrose/starch pathway related genes showed similar trends in both genotypes. In general, a higher response was recorded in 'Marte'. *Sus* isoforms (Fig. 6A-B) showed an opposite trend during water deficit. At t_{max} in WL plants, *Sus2* was strongly down regulated while *Sus3* was up regulated. An up regulation in 'Dvina' WL plants was observed only for *Sus2* gene at t_{rec}. The *Amy1.1-2* gene was more transcribed in both WL genotypes, mostly in 'Marte' (Fig. 7A). In contrast, *Bam5* was strongly transcribed in WL 'Marte' plants, but it did not elicit a water deficit response in 'Dvina' (Fig. 7B).

The other analysed genes showed a less marked response during water deficit. Moreover, *SS2* and *SS4* (Supplementary Fig. S4A-B, respectively) showed a weakly higher transcription at t_{max} in WL plants, especially *SS4*. In few cases, sucrose transporter genes *SUT2a-b*, *Suc2.1* and *SUT4* (Supplementary Fig. S5A-B-C, respectively) showed a slightly lower transcription in WL plants, especially *Suc.2.1* in 'Marte'. A schematic overview of experimental results is reported in Fig. 8.

DISCUSSION

Two genotypes *P. alba* 'Marte' and *P. deltoides* 'Dvina' showed different responses to cope with water deficit. This indicates that 'Marte' was more anisohydric than 'Dvina'. Water consuming strategy, which is typical of anisohydric plants under drought, was related to large differences between predawn and midday leaf water potentials and relative water contents (Attia *et al.*, 2015). In 'Marte,' this behaviour matched with the greatest plasticity in sucrose/starch pathway. Thus,

divergent strategies highlighted a different involvement of non-structural carbohydrates in drought tolerance of poplar. This further confirmed the fast growth recovery of 'Marte' after water deficit, which was related to variations in sugar metabolism. Soluble and stored carbohydrates did not represent a limiting factor for growth during water deficit. In 'Marte,' the increase of sucrose in xylem and the decrease of starch in xylem and sucrose in cambial region was a clear indication that non-structural carbohydrates were involved in osmotic adjustments. These changes mirrored those recorded for sucrose and starch in parenchyma cells during an embolism event, as reported by Secchi and Zwieniecki (2011) in *P. trichocarpa*, and Salleo *et al.* (2009) in *Laurus nobilis*. In fact, there was a correlation between soluble sugars and osmotically active compounds in xylem of 'Marte.' This highlights the importance of carbohydrates as active osmotic molecules, which were involved in eliciting water deficit response in this genotype. In 'Marte,' a high amount of soluble carbohydrates was present within the stem; however, soluble carbohydrates were not stored as starch. This represented an important bulk of carbon for supporting cambial cell divisions during recovery (Oribe *et al*., 2003). Water contained within phloem structures could be moved into xylem vessels to sustain transpiration stream and alleviate the risk of cavitation (Pfautsch *et al.*, 2015). In WW conditions, the higher bark RWC of 'Marte' might represent a reserve of water, which was more abundant than in 'Dvina.' This could be used during water deficit. Within xylem-phloem compartment, the high amount of water and carbohydrates contents was associated with the maintenance of stem elongation in 'Marte' during water deficit. Thus, in this genotype, primary meristems (apex) had a higher C-sink strength than cambial region under water deficit. However, the bark RWC decreased to 70% in both genotypes at t_{max}. This indicates that this level can represent a threshold value for the functionality of phloem in poplar species. In 'Marte,' osmotic adjustments were activated by decreasing water reserved within phloem. This was achieved by fluctuating stored and non-stored non-structural carbon compounds in xylem and cambial region. Mencuccini *et al.* (2013) proposed that osmotic potential of phloem can influence radial transfer of water and variations in bark thickness. The behaviour of 'Marte' confirmed a strong decrease in stem growth rate and an increase in instantaneous water deficit, which was mirrored by a decrease in sucrose content and $\Psi\pi_{sat}$ in cambial region.

In cambial region of 'Marte,' a high amount of soluble carbohydrates was associated with a higher transcription of the gene *Bam5*; this gene was involved in the degradation of starch. A very rapid carbon turnover was achieved consequently. The gene *Bam5* was overexpressed in several different starch-less mutants of *A. thaliana* (Monroe *et al*., 2014), indicating that different starch contents found in our contrasting genotypes can be strictly related to different transcription levels of this gene. In 'Marte,' *Bam5* gene transcription was increased strongly during water deficit and recovery.

This highlighted the probable pivotal function of this gene in different activation of osmotic adjustments fluctuating stored and non-stored non-structural carbohydrates. However, in both genotypes, starch was accumulated in the experimental period (from July to August) confirming that storage was not influenced by water deficit, but it was mainly driven by cambium phenology (Sauter and Van Cleve, 1994; Regier *et al.*, 2010).

A higher transcription of *Sus2* gene occurred after rehydration in 'Dvina.' This implies that C-fluxes were mainly directed towards cellulose production, corroborating the observation already made by Cocozza *et al.* (2011) in the same genotype under similar conditions. Konishi *et al.* (2004) and Coleman *et al.* (2009) proposed that *Sus2* isoform was responsible for directing carbon towards the cellulose biosynthesis in poplar species. In the long term, the high carbon investment into cell wall matrix, as recorded in 'Dvina', could reflect an increase in wood density. This induced a higher resistance to embolism formation and decreased the risk of cell wall collapse (Jacobsen *et al.*, 2005). However, wood density increased with respect to water deficit. This was also related to poor technological proprieties of newly produced wood (Cocozza *et al.*, 2011). The low wood density of 'Marte' was related to fast growth and more anisohydric behaviour of this genotype, which was also observed in a study conducted by Eller *et al.* (2018) on tropical trees. In 'Marte,' the difference between predawn and midday leaf water potentials and water contents was higher. This strongly decreased free water, which was available to support hydraulic network (α-α_f) in xylem. The high 'risk-taking' behaviour of 'Marte' under water deficit was coupled with similar carbohydrate variations, which was also observed in other woody plants during embolism response (Salleo *et al.*, 2009; Secchi and Zwieniecki, 2011; Attia *et al.*, 2015).

B-type cyclins regulated crucial checkpoint for mitosis (Fowler *et al.*, 1998), which was the primary activity in cambial region and the starting point of new xylem production (Larson, 1994). B-type cyclins was strongly down-regulated and carbohydrate content increased during water deficit. This confirmed that cell turgor prevented growth regardless of carbon supply (Palacio *et al.*, 2014). The assumption of no growth during stem shrinkage described as ZG-concept by Zweifel *et al.* (2016) was corroborated by synergic analyses of B-type cyclin transcription and stem radius variations. In fact, results confirmed that when stem did not grow ($\Delta SR/\Delta_t=0$), transcription levels of *CycB1.3-4* and *CycB2.1* genes were at detection limit.

In conclusion, the main physiological features were associated with different genotype-dependent responses. These features were related to the capacity to reallocate carbohydrates during water deficit. Moreover, the importance of cambial region activity under water deficit was clearly demonstrated and related to xylem traits. 'Marte' showed an active response and a fast recovery after water deficit, which was related to greater plasticity in sugar/starch conversion. In contrast,

less anisohydric behaviour was demonstrated by 'Dvina' during water deficit. This might be related to the impossibility of using carbohydrates in osmotic process. These carbohydrates were preferentially stored or used for cellulose production.

To elucidate plant responses to water deficit, it is necessary to understand how plant water status and leaf gas exchange can be integrated with the transportation of photoassimilate within phloem and xylem. Moreover, basic information is required about daily carbon balance and the limits of plants to shift energy among competing sinks under water limited conditions.

CONFLICTS OF INTEREST

The Authors have no conflicts of interest to declare.

SUPPLEMENTARY DATA

Table S1. List of primers used in this research.

Table S2. Glucose and fructose contents, glucose and fructose $\Psi\pi_{sat}$ in the cambial region and the xylem.

Fig. S1. Calculation of the instantaneous stem water deficit.

Fig. S2. Starch localization by Lugol's solution.

Fig. S3. Osmotically active molecules in cambial region and xylem.

Fig. S4. mRNA accumulations of *SS2* and *SS4* genes.

Fig. S5. mRNA accumulations of *SUT2*, *Suc2.1*, and *SUT4* genes.

AKNOWLEDGMENTS

Financial support was provided by Regione Toscana (POR CRO FSE 2012-2014, research project "Sysbiofor") to Alessio Giovannelli, by Fondazione Cassa di Risparmio di Lucca (project "Physiological parameters for the selection of poplar genotypes with enhanced resistance to water stress for the exploitation of marginal areas) to Carlo Sorce, and by Agrobioscience PhD program at Scuola Superiore Sant'Anna of Pisa for granting Silvia Traversari scholarship. The authors would like to extend their sincere thanks to Mrs Monica Anichini for histological observations and Ms Maria Giustina Rotordam for sample preparation.

REFERENCES

Adams HD, Germino MJ, Breshears DD, Barron-Gafford GA, Guardiola-Claramonte M, Zou CB, Huxman TE. 2013. Nonstructural leaf carbohydrate dynamics of *Pinus edulis* during

drought-induced tree mortality reveal role for carbon metabolism in mortality mechanism. New Phytologist **197**, 1142–51.

Anderegg WR, Berry JA, Field CB. 2012. Linking definitions, mechanisms and modelling of drought-induced tree death. Trend Plant Science **17**, 693–700

Arend M, Fromm J. 2007. Seasonal change in the drought response of wood cell development in poplar. Tree Physiology **27**, 985–992.

Attia Z, Domec JC, Oren R, Way DA, Moshelion M. 2015. Growth and physiological responses of isohydric and anisohydric poplars to drought. Journal of Experimental Botany **66**, 4373–4381.

Bae EK, Lee H, Lee JS, Noh EW. 2010. Isolation and characterization of osmotic stress-induced genes in poplar cells by suppression subtractive hybridization and cDNA microarray analysis. Plant Physiology and Biochemistry **48**, 136–141.

Berry SL, Roderick ML. 2005. Plant–water relations and the fibre saturation point. New Phytologist **168**, 25–37.

Blum A. 2017. Osmotic adjustment is a prime drought stress adaptive engine in support of plant production. Plant, Cell & Environment **40**, 4–10.

Brunner AM, Yakovlev IA, Strauss SH. 2004. Validating internal controls for quantitative plant gene expression studies. BMC Plant Biology **4**, 14.

Carriero G, Emiliani G, Giovannelli A, Hoshika Y, Manning WJ, Traversi ML, Paoletti E. 2015. Effects of long-term ambient ozone exposure on biomass and wood traits in poplar treated with ethylenediurea (EDU). Environmental Pollution **206**, 575–581.

Chang S, Puryear J, Cairney J. 1993. A simple and efficient method for isolating RNA from pine trees. Plant Molecular Biology Reporter **11**, 113–116.

Cocozza C, Giovannelli A, Traversi ML, Castro G, Cherubini P, Tognetti R. 2011. Do tree-ring traits reflect different water deficit responses in young poplar clones (*Populus* × *canadensis* Mönch 'I-214' and *P. deltoides* 'Dvina')? Trees **25**, 975–985.

Coleman HD, Yan J, Mansfield SD. 2009. Sucrose synthase affects carbon partitioning to increase cellulose production and altered cell wall ultrastructure. PNAS **106**, 13118–13123.

Diaz-Espejo A, Hernandez-Santana V. 2017. The phloem–xylem consortium: until death do them part. Tree physiology **37**, 847–850.

Edgar RC. 2004. MUSCLE: multiple sequence alignment with high accuracy and high throughput. Nucleic Acids Research **32**, 1792–1797.

Fowler MR, Eyre S, Scott NW, Slater A, Elliott MC. 1998. The plant cell cycle in context. Molecular Biotechnology **10**, 123–153.

Emiliani G, Traversari S, De Carlo A, Traversi ML, Cantini C, Giovannelli A. 2016. B-type cyclin modulation in response to carbon balance in callus of *Populus alba*. Plant Cell, Tissue and Organ Culture **124**, 283–293.

Eller CB, Barros FV, Bittencourt PRL, Rowland L, Mencuccini M, Olivei RS. 2018. Xylem hydraulic safety and construction costs determine tropical tree growth. Plant, Cell & Environment **41**, 548–562.

Galvez DA, Landhäusser SM, Tyree MT. 2011. Root carbon reserve dynamics in aspen seedlings: does simulated drought induce reserve limitation?. Tree Physiology **31**, 250–257.

Giovannelli A, Emiliani G, Traversi ML, Deslauriers A, Rossi S. 2011. Sampling cambial region and mature xylem for non structural carbohydrates and starch analyses. Dendrochronologia **29**, 177–182.

Gucci R, Lombardini L, Tattini M. 1997. Analysis of leaf water relations in leaves of two olive (*Olea europaea*) cultivars differing in tolerance to salinity. Tree Physiology **17**, 13–21.

Konishi T, Ohmiya Y, Hayashi T. 2004. Evidence that sucrose loaded into the phloem of a poplar leaf is used directly by sucrose synthase associated with various β-glucan synthases in the stem. Plant Physiology **134**, 1146–1152.

Korner C. 2015. Paradigm shift in plant growth control. Current Opinion in Plant Biology **25**, 107–114.

Jacobsen AL, Ewers FW, Pratt RB, Paddock WA, Davis SD. 2005. Do xylem fibers affect vessel cavitation resistance?. Plant physiology **139**, 546–556.

Harris DC. 1997. Internal standards. In: Quantitative chemical analysis, 5th edn. New York: W.H. Freeman and Company 104.

Hartmann H. 2015. Carbon starvation during drought-induced tree mortality – are we chasing a myth? Journal of Plant Hydraulics **2**, e-005.

Haworth M, Centritto M, Giovannelli A, Marino G, Proietti N, Capitani D, De Carlo A, Loreto F. 2017. Xylem morphology determines the drought response of two *Arundo donax* ecotypes from contrasting habitats. Global Change Biology Bioenergy **9**, 119–131.

Huala E, Dickerman AW, Garcia-Hernandez M, *et al.* 2001. The Arabidopsis Information Resource (TAIR): a comprehensive database and web-based information retrieval, analysis, and visualization system for a model plant. Nucleic Acids Research **29**, 102–105.

Lachenbruch B, McCulloh KA. 2014. Traits, properties, and performance: how woody plants combine hydraulic and mechanical functions in a cell, tissue, or whole plant. New Phytologist **204**, 747–764.

Larson PR. 1994. The vascular cambium. Springer, Berlin, Heidelberg.

Lintunen A, Paljakka T, Jyske T, *et al*. 2016. Osmolality and non-structural carbohydrate composition in the secondary phloem of trees across a latitudinal gradient in Europe. Frontiers in Plant Science **7**, 726.

Luisi A, Giovannelli A, Traversi ML, Anichini M, Sorce C. 2014. Hormonal responses to water deficit in cambial tissues of *Populus alba* L. Journal of Plant Growth Regulation **33**, 489–498.

Mencuccini M, Hölttä T, Sevanto S, Nikinmaa E. 2013. Concurrent measurements of change in the bark and xylem diameters of trees reveal a phloem-generated turgor signal. New Phytologist **198**, 1143–1154.

Monclus R, Villar M, Barbaroux C, *et al*. 2009. Productivity, water-use efficiency and tolerance to moderate water deficit correlate in 33 poplar genotypes from a *Populus deltoides* × *Populus trichocarpa* F1 progeny. Tree Physiology **29**, 1329–1339.

Monroe JD, Storm AR, Badley EM, Lehman MD, Platt SM, Saunders LK, Schmitz JM, Torres CE. 2014. β-Amylase1 and β-amylase3 are plastidic starch hydrolases in Arabidopsis that seem to be adapted for different thermal, pH, and stress conditions. Plant physiology **166**, 1748–1763.

Oribe Y, Funada R, Kubo T. 2003. Relationships between cambial activity, cell differentiation and the localization of starch in storage tissues around the cambium in locally heated stems of *Abies sachalinensis* (Schmidt) Masters. Trees-Structure and Function **17**, 185–192.

Palacio S, Hoch G, Sala A, Korner C, Millard P. 2014. Does carbon storage limit tree growth? New Phytologist **201**, 1096–1100.

Pallara G, Giovannelli A, Traversi ML, Camussi A, Racchi ML. 2012. Effect of water deficit on expression of stress-related genes in the cambial region of two contrasting poplar clones. Journal of Plant Growth Regulation **31**, 102–112.

Pfaffl MW. 2001. A new mathematical model for relative quantification in real-time RT-PCR. Nucleic Acids Research **29**, e45.

Pfautsch S, Renard J, Tjoelker MG, Salih A. 2015. Phloem as capacitor: radial transfer of water into xylem of tree stems occurs via symplastic transport in ray parenchyma. Plant Physiology **167**, 963–971.

Regier N, Streb S, Zeeman SC, Frey B. 2010. Seasonal changes in starch and sugar content of poplar (*Populus deltoides* × *nigra* cv. Dorskamp) and the impact of stem girdling on carbohydrate allocation to roots. Tree Physiology **30**, 979–987.

Roderick ML, Berry SL. 2001. Linking wood density with tree growth and environment: a theoretical analysis based on the motion of water. New Phytologist **149**, 473–485.

Rosner S. 2017. Wood density as a proxy for vulnerability to cavitation: size matters. Journal of Plant Hydraulics **4**, e-001.

Sala A, Woodruff DR, Meinzer FC. 2012. Carbon dynamics in trees: feast or famine?. Tree Physiology **32**, 764–775.

Salleo S, Trifilò P, Esposito S, Nardini A, Lo Gullo MA. 2009. Starch-to-sugar conversion in wood parenchyma of field-growing *Laurus nobilis* plants, a component of the signal pathway for embolism repair? Functional Plant Biology **36**, 815–825.

Santos MG, Pimentel C. 2009. Daily balance of leaf sugars and amino acids as indicators of common bean (*Phaseolus vulgaris* L.) metabolic response and drought intensity. Physiology and Molecular Biology of Plants **15**, 23–30.

Sauter JJ, Van Cleve B. 1994. Storage, mobilization and interrelations of starch, sugars, protein and fat in the ray storage tissue of poplar trees. Trees **8**, 297–304.

Secchi F, Zwieniecki MA. 2011. Sensing embolism in xylem vessels: the role of sucrose as a trigger for refilling. Plant, Cell & Environment **34**, 514–524.

Sengupta S, Majumdar AL. 2014. Physiological and genomic basis of mechanical-functional trade-off in plant vasculature. Frontiers in Plant Science **28**, 224.

Sevanto S, McDowell NG, Dickman LT, Pangle R, Pockman WT. 2014. How do trees die? A test of the hydraulic failure and carbon starvation hypotheses. Plant, Cell & Environment **37**, 153–161.

Shao HB, Chu LY, Jaleel CA, Zhao CX. 2008. Water-deficit stress-induced anatomical changes in higher plants. Comptes Rendus Biologies **331**, 215–225.

Sjödin A, Street NR, Sandberg G, Gustafsson P, Jansson S. 2009. PopGenIE: The *Populus* Genome Integrative Explorer. A new tool for exploring the *Populus* genome. New Phytologist **182**, 1013–1025.

Sorce C, Giovannelli A, Sebastiani L, Anfodillo T. 2013. Hormonal signals involved in the regulation of cambial activity, xylogenesis and vessel patterning in trees. Plant Cell Report **32**, 885–898.

Spicer R. 2014. Symplasmic networks in secondary vascular tissues: parenchyma distribution and activity supporting long-distance transport. Journal of Experimental Botany **65**, 1829–1848.

Streb S, Zeeman SC. 2012. Starch metabolism in Arabidopsis. The Arabidopsis Book **10**, e0160.

Street NR, Skogström O, Sjödin A, Tucker J, Rodríguez□Acosta M, Nilsson P, Jansson S, Taylor G. 2006. The genetics and genomics of the drought response in *Populus*. The Plant Journal **48**, 321–341.

Tamura K, Peterson D, Peterson N, Stecher G, Nei M, Kumar S. 2011. MEGA5: molecular evolutionary genetics analysis using maximum likelihood, evolutionary distance, and maximum parsimony methods. Molecular Biology and Evolution **28**, 2731–2739.

Osakabe Y, Osakabe K, Shinozaki K, Tran LSP. 2014. Response of plants to water stress. Frontiers in Plant Science **5**, 86.

Uggla C, Sundberg B. 2002. Sampling of cambial region tissues for high resolution analysis. In: Chaffey, N.J. (Ed.), Wood Formation in Trees. Cell and Molecular Biology Techniques. Taylor & Francis, New York, 215–228.

Yin C, Duan B, Wang X, Lia C. 2004. Morphological and physiological responses of two contrasting poplar species to drought stress and exogenous abscisic acid application. Plant Science **167**, 1091–1097.

Yin C, Wang X, Duan B, Luo J, Lia C. 2005. Early growth, dry matter allocation and water use efficiency of two sympatric *Populus* species as affected by water stress. Environmental and Experimental Botany **53**, 315–322.

Zhang D, Xu B, Yang X, Zhang Z, Li B. 2011. The sucrose synthase gene family in *Populus*: structure, expression, and evolution. Tree Genetics & Genomes **7**, 443–456.

Zweifel R, Haeni M, Buchmann N, Eugster W. 2016. Are trees able to grow in periods of stem shrinkage?. New Phytologist **211**, 839–849.

Zwieniecki MA, Secchi F. 2015. Threats to xylem hydraulic function of trees under ‘new climate normal’ conditions. Plant, Cell & Environment **38**, 1713–1724.

Table 1. Sucrose and starch content, sucrose $\Psi\pi_{sat}$, and sucrose/starch ratio in cambial region and xylem of *P. deltoides* 'Dvina' and *P. alba* 'Marte' at t_0 (0 d), after 8 d from withholding of water (t_{max}) and 13 d after resumption of irrigation (t_{rec}). The values represent the mean of four biological replicates ± SD. Data were analysed with *t*-test (t_0) or two-way ANOVA (t_{max} and t_{rec}). The means were compared by following a LSD Fisher test. Different letters indicate significant differences ($P < 0.05$). WW, well-watered; WL, water limited. ns, not significant; *$P < 0.05$; **$P < 0.01$; ***$P < 0.001$.

Parameter	Genotype (G)						
	'Dvina'		'Marte'				
	Water Regime (WR)						
	WW		WW				
t_0	*Cambial Region*				*t*-test		
Starch (mg g^{-1} DW)	109.3±20.4		11.6±2.7		***		
Sucrose (mg g^{-1} DW)	84.8±14.3		93.7±33.3		ns		
$\Psi\pi_{sat}$ sucrose (MPa)	-0.23±0.02		-0.21±0.05		ns		
Sucrose/Starch	0.9±0.2		6.2±2.5		ns		
	Xylem						
Starch (mg g^{-1} DW)	10.0±1.4		3.6±2.3		**		
Sucrose (mg g^{-1} DW)	21.9±6.2		21.6±3.1		ns		
$\Psi\pi_{sat}$ sucrose (MPa)	-0.08±0.02		-0.06±0.01		ns		
Sucrose/Starch	2.2±0.6		7.4±3.7		ns		
	'Dvina'		'Marte'		ANOVA		
	WW	WL	WW	WL	WR	G	WR *x* G
t_{max}	*Cambial Region*						
Starch (mg g^{-1} DW)	79.9±46.0	51.2±12.9	18.2±7.6	34.9±18.1	ns	**	ns
Sucrose (mg g^{-1} DW)	50.0±13.2 b	60.3±12.4 ab	73.6±12.0 a	55.2±7.7 b	ns	ns	*
$\Psi\pi_{sat}$ sucrose (MPa)	-0.15±0.04 b	-0.18±0.04 ab	-0.21±0.03 a	-0.16±0.02 b	ns	ns	*
Sucrose/Starch	0.9±0.6 b	1.2±0.3 b	4.4±1.1 a	2.0±1.1 b	*	***	**
	Xylem						
Starch (mg g^{-1} DW)	9.7±2.5	8.2±1.9	7.9±1.8	3.9±1.7	*	*	ns
Sucrose (mg g^{-1} DW)	20.5±3.9	22.8±2.8	22.1±4.7	29.8±1.7	*	*	ns
$\Psi\pi_{sat}$ sucrose (MPa)	-0.08±0.01	-0.08±0.01	-0.06±0.01	-0.09±0.00	*	ns	ns
Sucrose/Starch	2.0±0.7 b	2.9±0.8 b	2.9±0.9 b	8.6±3.3 a	**	**	*
t_{rec}	*Cambial Region*						
Starch (mg g^{-1} DW)	95.84±25.0	70.4± 26.2	13.8±13.2	39.0±18.7	ns	**	ns
Sucrose (mg g^{-1} DW)	61.6±14.7 c	80.3±12.5 b	100.5±15.7 a	76.9±9.8 bc	ns	*	*
$\Psi\pi_{sat}$ sucrose (MPa)	-0.18±0.04 b	-0.23±0.04 ab	-0.28±0.04 a	-0.22±0.03 ab	ns	ns	*
Sucrose/Starch	0.7±0.3 b	1.3±0.6 b	11.5±6.7 a	2.2±0.7 b	*	**	*
	Xylem						
Starch (mg g^{-1} DW)	19.9±2.7	24.1±1.8	12.1±1.4	14.4±4.2	*	***	ns
Sucrose (mg g^{-1} DW)	23.8±9.0	14.6±2.7	19.7±2.6	19.0±2.7	ns	ns	ns
$\Psi\pi_{sat}$ sucrose (MPa)	-0.09±0.03	-0.05±0.01	-0.06±0.01	-0.05±0.01	ns	ns	ns
Sucrose/Starch	1.2±0.5	0.6±0.5	1.7±0.4	1.4±0.4	*	**	ns

Table 2. Water potential difference between predawn and midday ($\Delta\Psi w_{pd\text{-}md}$, MPa), instantaneous water use efficiency (WUE*i*, mmol CO_2 mol^{-1} H_2O), leaf water content difference between predawn and midday ($\Delta LWC_{pd\text{-}md,}$ %), specific leaf area (SLA, m^2 kg^{-1}), and the amount of free water available to support hydraulic network (α-α_f) of *P. deltoides* 'Dvina' and *P. alba* 'Marte' at t_{max}. The values represent the mean of four biological replicates ± SD. Data were analysed with two-way ANOVA. The means were compared by following a LSD Fisher test. Different letters indicate significant differences ($P < 0.05$). WW, well-watered; WL, water limited; ns, not significant; *$P < 0.05$; **$P < 0.01$; ***$P < 0.001$.

Parameter	Genotype (G)				ANOVA		
	'Dvina'		'Marte'				
	Water Regime (WR)						
	WW	WL	WW	WL	WR	G	WR *x* G
$\Delta\Psi w_{pd\text{-}md}$	1.2±0.1 a	0.5±0.2 b	1.2±0.1 a	0.1± 0.1 c	***	*	*
WUE*i*	1.2±0.1	0.2±0.0	1.4±0.1	0.4± 0.3	***	ns	ns
$\Delta LWC_{pd\text{-}md}$	5.1±0.3 b	6.6±4.0 b	37.4±3.9 a	0.0±6.5 b	***	**	***
SLA	9.6±1.0	10.6±1.8	12.7±1.0	12.5±1.1	ns	***	ns
α-α_f	1.03±0.10 a	0.44±0.07 b	1.05±0.06 a	0.30±0.01 c	***	ns	*

FIGURE LEGENDS

Fig. 1. Diagram of 21 days of experimental plane with *P. deltoides* 'Dvina' clone and *P. alba* 'Marte' clone. Plant samplings were made at t_0 (0 d, n = 3), after 8 d from withholding of water (t_{max}, n = 4), and 13 d after resumption of irrigation (t_{rec}, n = 4). Meteorological data are reported in the figure.

Fig. 2. Stem growth rate ($\Delta SR/\Delta_t$) (A) and instantaneous stem water deficit (ΔW) (B) of *P. deltoides* clone 'Dvina' and *P. alba* clone 'Marte' subjected to 8 d of water deficit. Data were compared between genotypes and treatments at t_0 (0 d), after 8 d from withholding of water (t_{max}), and 13 d after resumption of irrigation (t_{rec}). The bars represent the mean of four biological replicates (± SD). Data were analysed with *t*-test (t_0) or two-way ANOVA (t_{max} and t_{rec}). Significant differences are reported in bold. The means were compared by following a LSD Fisher test. Different letters indicate significant differences ($P < 0.05$).

Fig. 3. Bark (A) and xylem (B) relative water contents of *P. deltoides* clone 'Dvina' and *P. alba* clone 'Marte' at t_0 (0 d), after 8 d from withholding of water (t_{max}), and 13 d after resumption of irrigation (t_{rec}). The bars represent the mean of four biological replicates (± SD). For the statistical analyses, the percentages were subjected to arcsin transformation (arcsin $\sqrt{x}$). Data were analysed with *t*-test (t_0) or two-way ANOVA (t_{max} and t_{rec}). Significant differences are reported in bold. The means were compared by following a LSD Fisher test. Different letters indicate significant differences ($P < 0.05$).

Fig. 4. Relative extractable water (REW) in the substrate of *P. deltoides* clone 'Dvina' and *P. alba* clone 'Marte' during the experiment. The values were referred at t_0 (0 d), after 8 d from withholding of water (t_{max}), and 13 d after resumption of irrigation (t_{rec}). The values represent the mean of four biological replicates (± SD).

Fig. 5. mRNA accumulations of *CycB1.3-4* (A) and *CycB2.1* (B) genes in cambial region of *P. deltoides* 'Dvina' and *P. alba* 'Marte' at t_0 (0 d), after 8 d from withholding of water (t_{max}), and 13 d after resumption of irrigation (t_{rec}). The bars represent the mean of three biological replicates (+ SD). Data were analysed with *t*-test (t_0) or two-way ANOVA (t_{max} and t_{rec}). Significant differences are reported in bold. The means were compared by following a LSD Fisher test. Different letters indicate significant differences ($P < 0.05$).

Fig. 6. mRNA accumulations of *Sus2* (A) and *Sus3* (B) genes in cambial region of *P. deltoides* 'Dvina' and *P. alba* 'Marte' at t_0 (0 d), after 8 d from withholding of water (t_{max}), and 13 d after resumption of irrigation (t_{rec}). The bars represent the mean of three biological replicates + SD. Data were analysed with *t*-test (t_0) or two-way ANOVA (t_{max} and t_{rec}). Significant differences are reported in bold. The means were compared by following a LSD Fisher test. Different letters indicate significant differences ($P < 0.05$).

Fig. 7. mRNA accumulations of *Amy1.1-2* (A) and *Bam5* (B) genes in cambial region of *P. deltoides* 'Dvina' and *P. alba* 'Marte' a at t_0 (0 d), after 8 d from withholding of water (t_{max}), and 13 d after resumption of irrigation (t_{rec}). The bars represent the mean of three biological replicates + SD. Data were analysed with *t*-test (t_0) or two-way ANOVA (t_{max} and t_{rec}). Significant differences are reported in bold. The means were compared by following a LSD Fisher test. Different letters indicate significant differences ($P < 0.05$).

Fig. 8. Schematic overview of experimental results on *P. deltoides* 'Dvina' and *P. alba* 'Marte' at t_0 (0 d), after 8 d from withholding of water (t_{max}), and 13 d after resumption of irrigation (t_{rec}). CR, cambial region; X, xylem. WW, well-watered; WL, water limited.

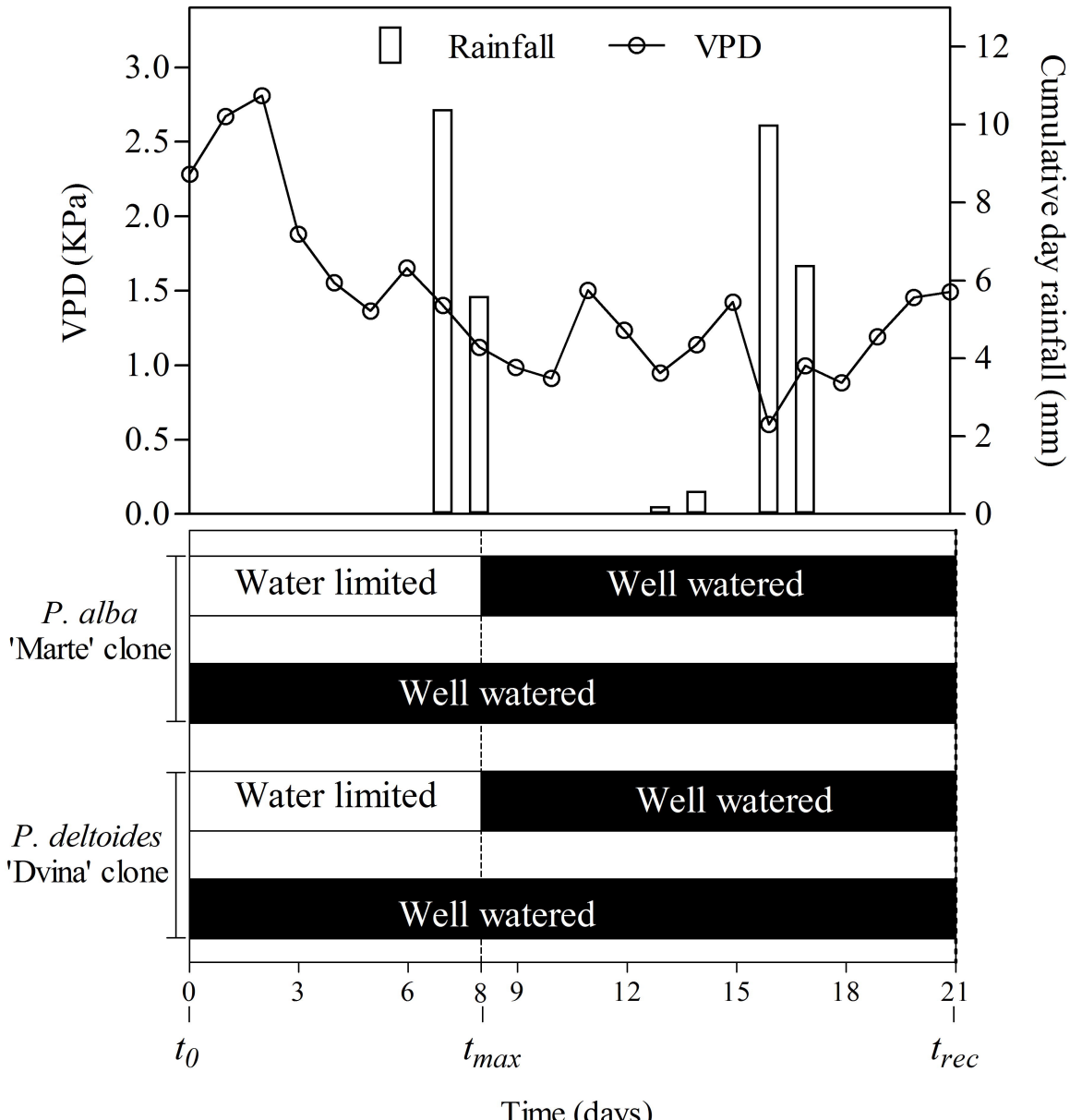
Rainfall
VPD
VPD (KPa)
Cumulative day rainfall (mm)
3.0
2.5
2.0
1.5
1.0
0.5
0.0
12
10
8
6
4
2
0
P. alba
'Marte' clone
Water limited
Well watered
Well watered
P. deltoides
'Dvina' clone
Water limited
Well watered
Well watered
0
3
6
8
9
12
15
18
21
t0
tmax
trec
Time (days)

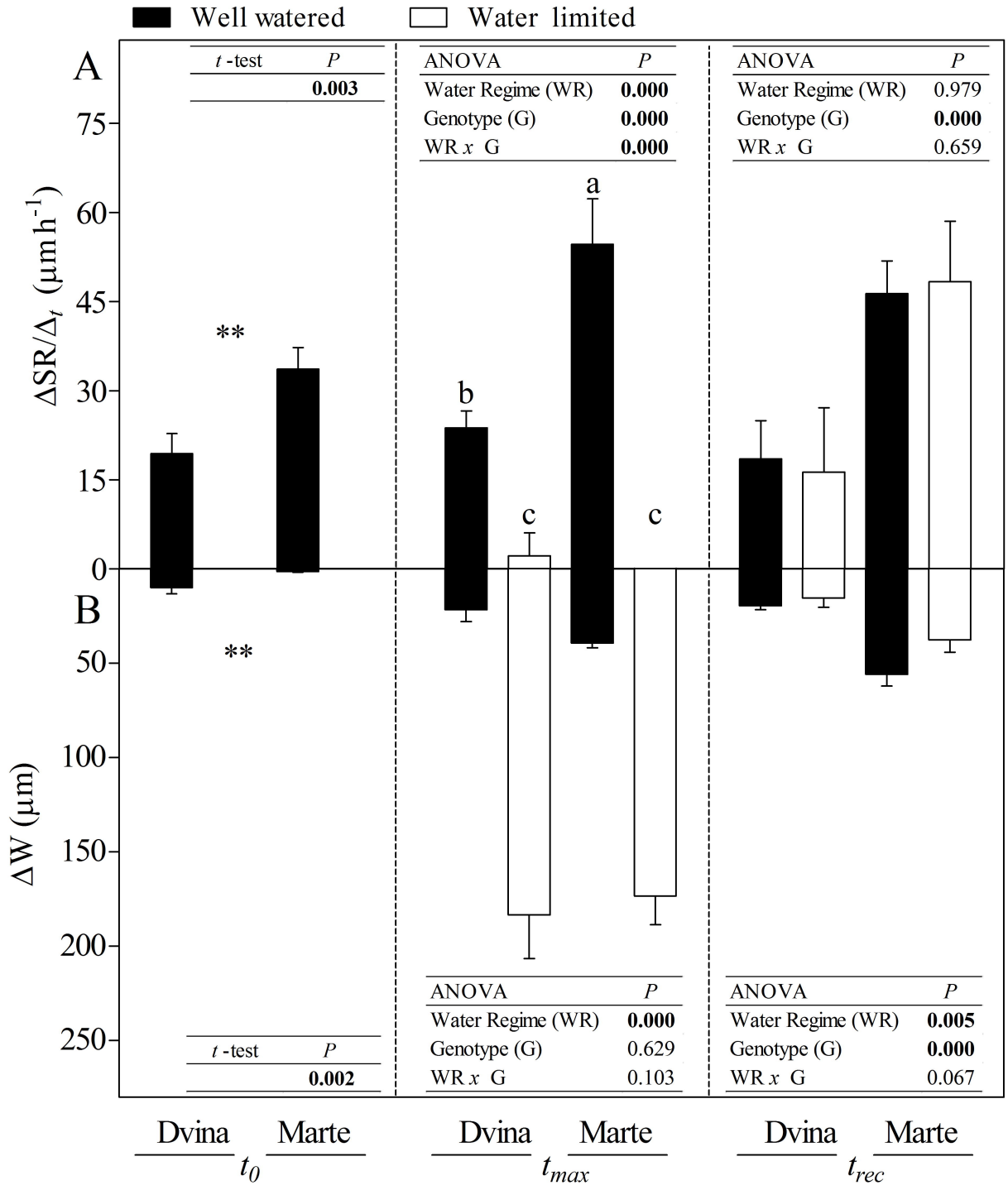
Well watered
Water limited
A
B
ΔSR/Δt (μm h-1)
ΔW (μm)
75
60
45
30
15
0
50
100
150
200
250
**
**
a
b
c
c
t -test P
0.003
t -test P
0.002
ANOVA P
Water Regime (WR) 0.000
Genotype (G) 0.000
WR x G 0.000
ANOVA P
Water Regime (WR) 0.000
Genotype (G) 0.629
WR x G 0.103
ANOVA P
Water Regime (WR) 0.979
Genotype (G) 0.000
WR x G 0.659
ANOVA P
Water Regime (WR) 0.005
Genotype (G) 0.000
WR x G 0.067
Dvina
Marte
t0
Dvina
Marte
tmax
Dvina
Marte
trec

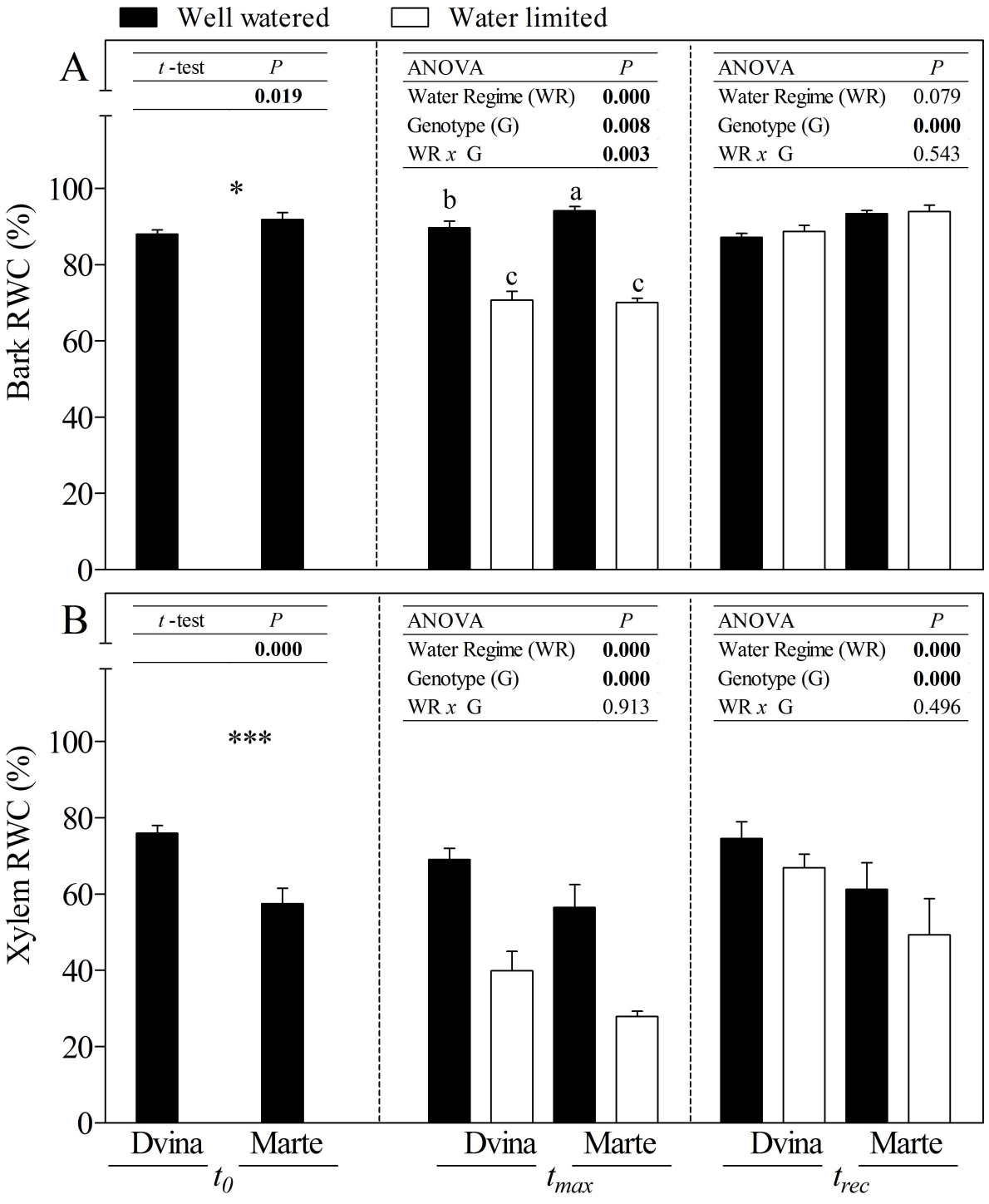
Well watered
Water limited
A
t -test P
0.019
*
ANOVA P
Water Regime (WR) 0.000
Genotype (G) 0.008
WR x G 0.003
b
a
c
c
ANOVA P
Water Regime (WR) 0.079
Genotype (G) 0.000
WR x G 0.543
Bark RWC (%)
100
80
60
40
20
0
B
t -test P
0.000
***
ANOVA P
Water Regime (WR) 0.000
Genotype (G) 0.000
WR x G 0.913
ANOVA P
Water Regime (WR) 0.000
Genotype (G) 0.000
WR x G 0.496
Xylem RWC (%)
100
80
60
40
20
0
Dvina
Marte
Dvina
Marte
Dvina
Marte
t0
tmax
trec

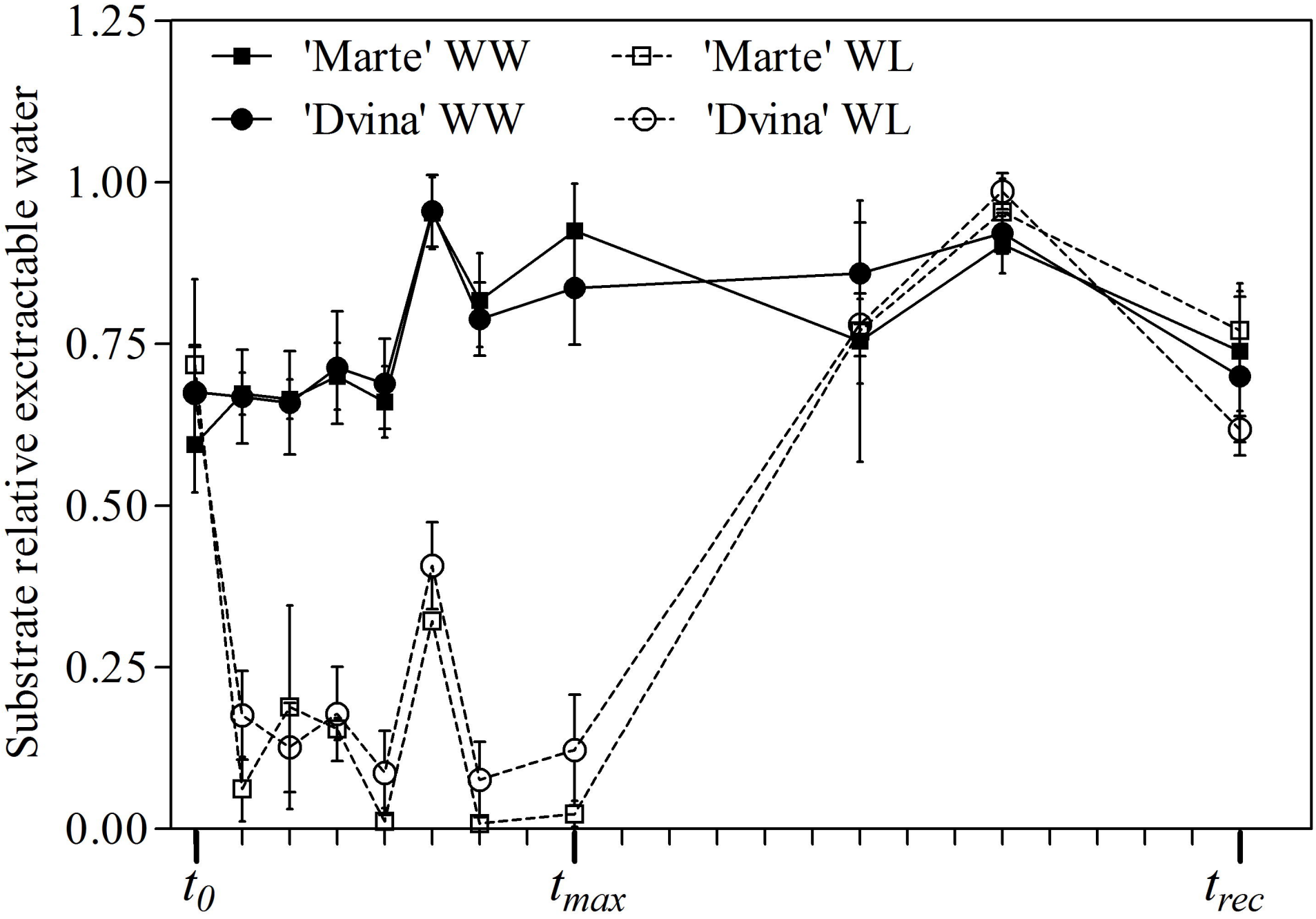
'Marte' WW
'Marte' WL
'Dvina' WW
'Dvina' WL
Substrate relative exctractable water
1.25
1.00
0.75
0.50
0.25
0.00
t_0
t_{max}
t_{rec}

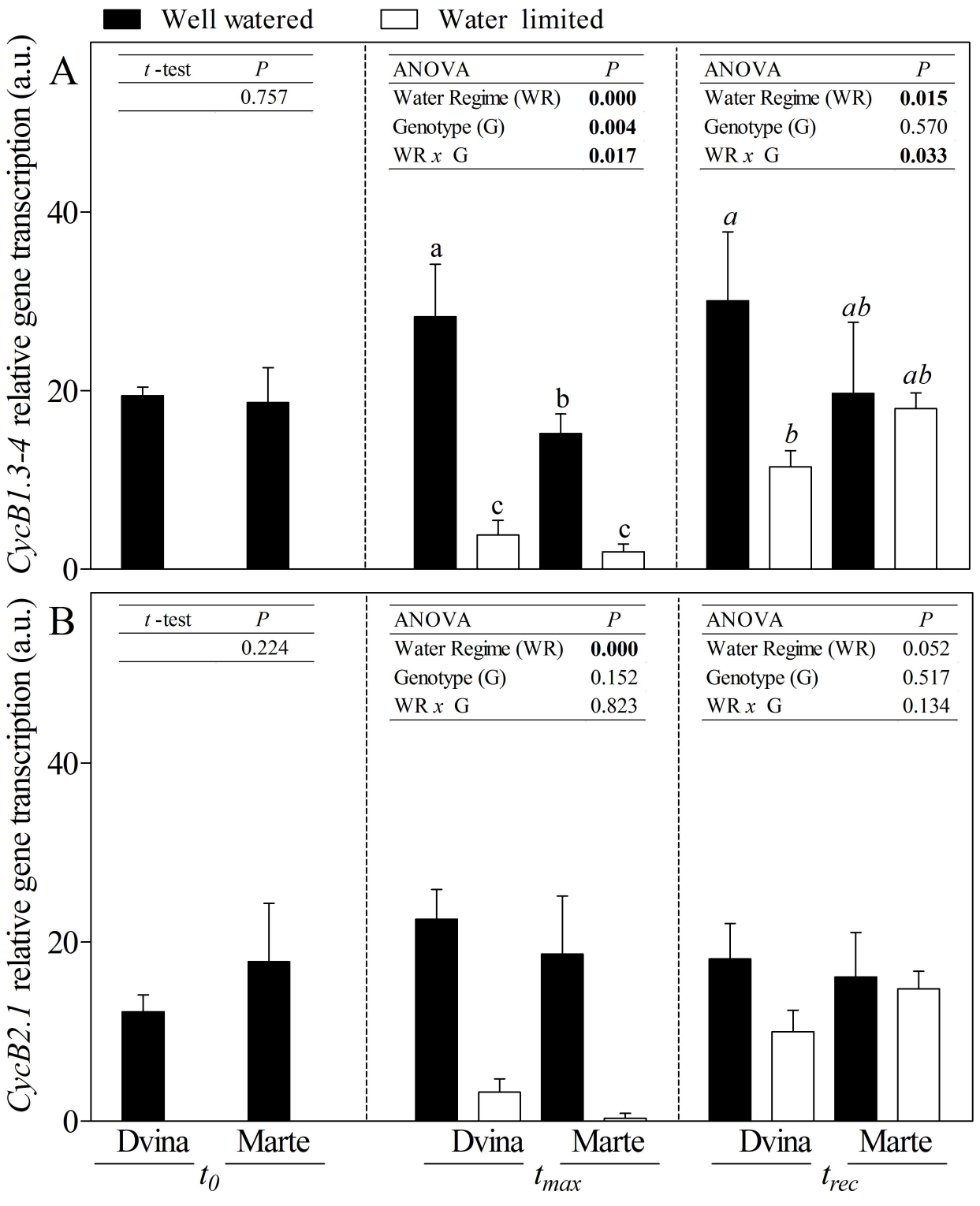
Well watered
Water limited
A
B
CycB1.3-4 relative gene transcription (a.u.)
CycB2.1 relative gene transcription (a.u.)
0
20
40
t-test P
0.757
ANOVA P
Water Regime (WR) 0.000
Genotype (G) 0.004
WR x G 0.017
ANOVA P
Water Regime (WR) 0.015
Genotype (G) 0.570
WR x G 0.033
a
c
b
c
a
b
ab
ab
t-test P
0.224
ANOVA P
Water Regime (WR) 0.000
Genotype (G) 0.152
WR x G 0.823
ANOVA P
Water Regime (WR) 0.052
Genotype (G) 0.517
WR x G 0.134
Dvina
Marte
Dvina
Marte
Dvina
Marte
t0
tmax
trec

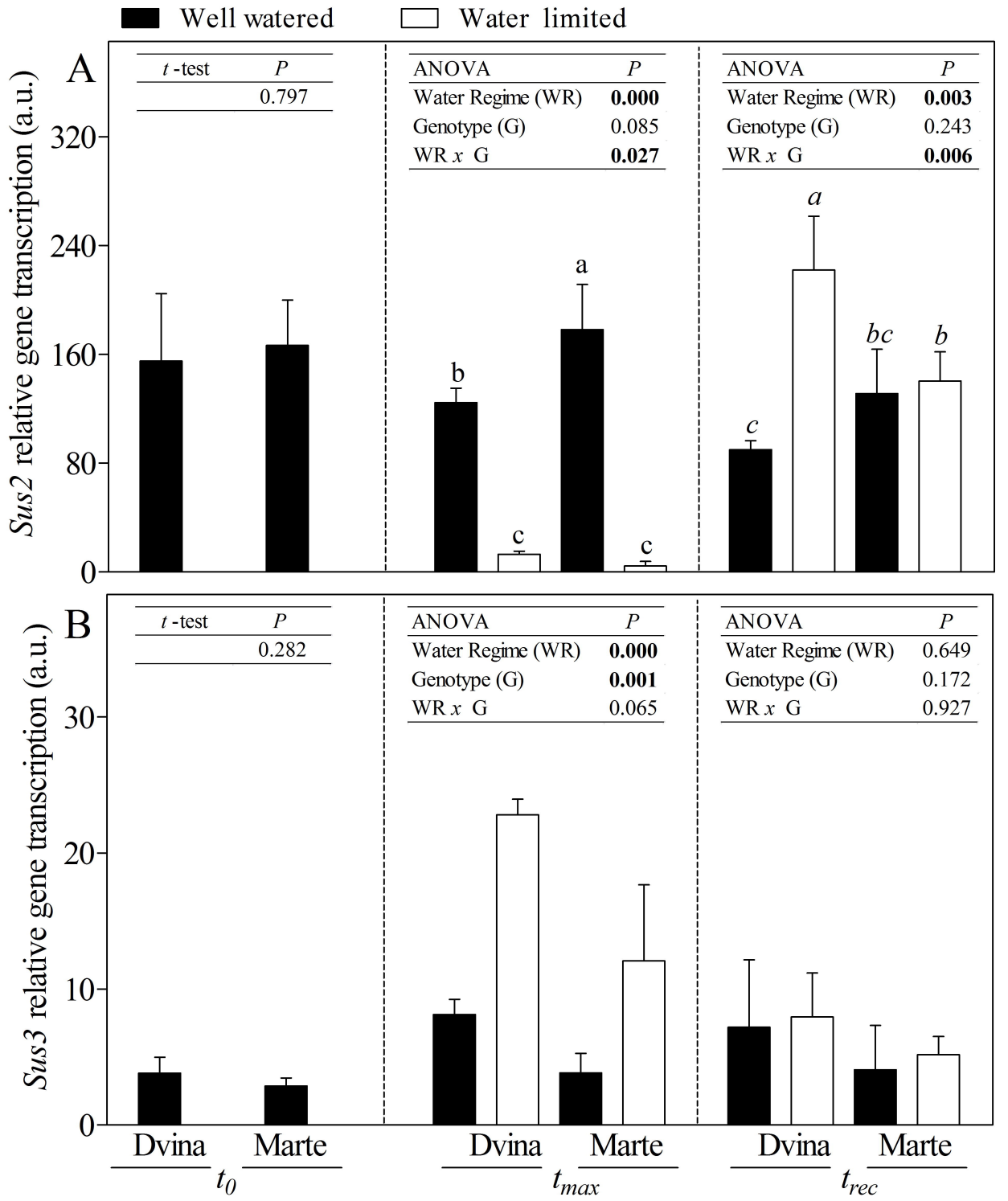
Well watered
Water limited
A
Sus2 relative gene transcription (a.u.)
t -test P
0.797
ANOVA P
Water Regime (WR) 0.000
Genotype (G) 0.085
WR x G 0.027
ANOVA P
Water Regime (WR) 0.003
Genotype (G) 0.243
WR x G 0.006
320
240
160
80
0
b
c
a
c
c
a
bc
b
B
Sus3 relative gene transcription (a.u.)
t -test P
0.282
ANOVA P
Water Regime (WR) 0.000
Genotype (G) 0.001
WR x G 0.065
ANOVA P
Water Regime (WR) 0.649
Genotype (G) 0.172
WR x G 0.927
30
20
10
0
Dvina
Marte
Dvina
Marte
Dvina
Marte
t0
tmax
trec

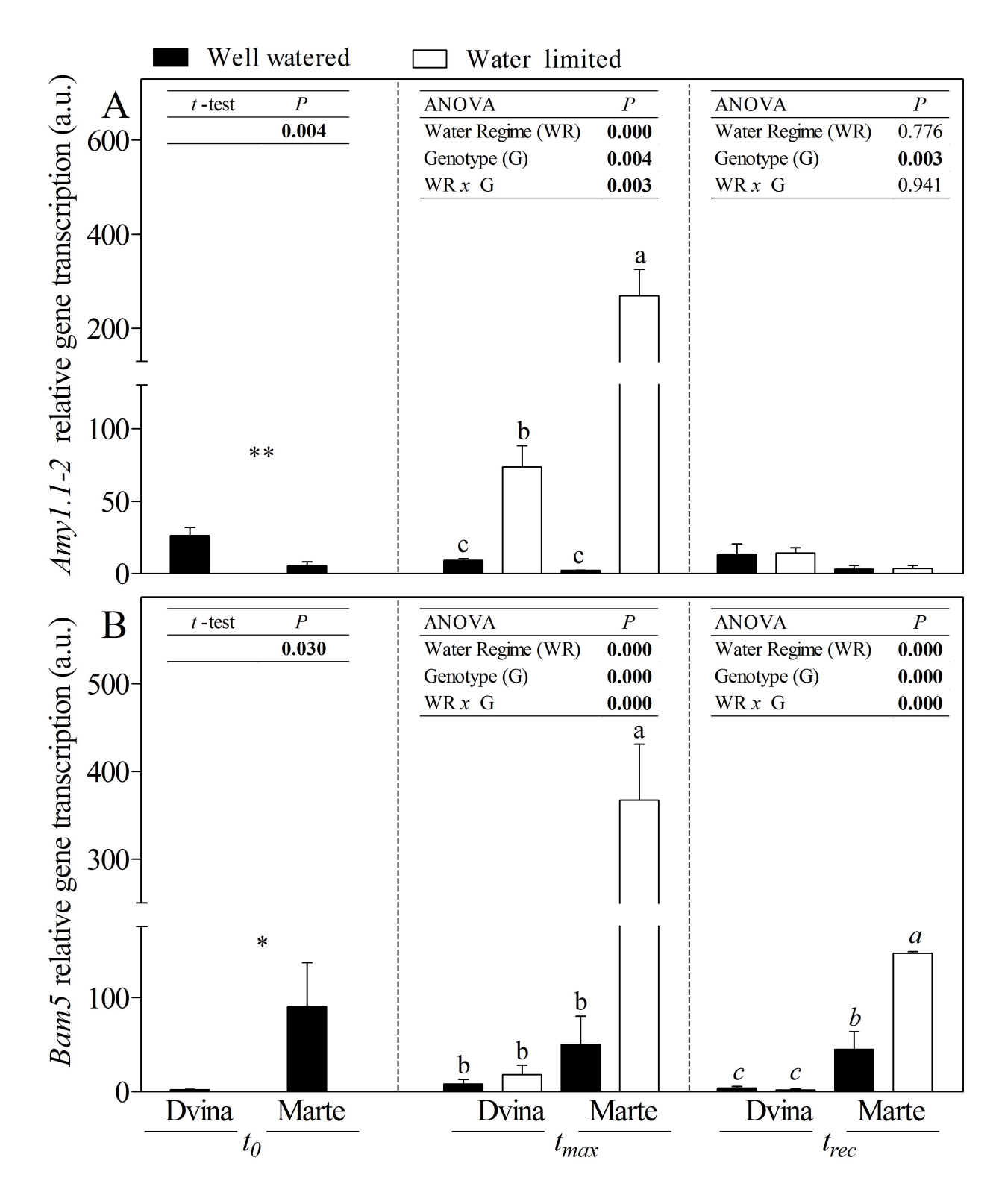
Well watered
Water limited
A
Amy1.1-2 relative gene transcription (a.u.)
t -test P
0.004
ANOVA P
Water Regime (WR) 0.000
Genotype (G) 0.004
WR x G 0.003
ANOVA P
Water Regime (WR) 0.776
Genotype (G) 0.003
WR x G 0.941
**
B
Bam5 relative gene transcription (a.u.)
t -test P
0.030
ANOVA P
Water Regime (WR) 0.000
Genotype (G) 0.000
WR x G 0.000
ANOVA P
Water Regime (WR) 0.000
Genotype (G) 0.000
WR x G 0.000
*
Dvina
Marte
t0
tmax
trec

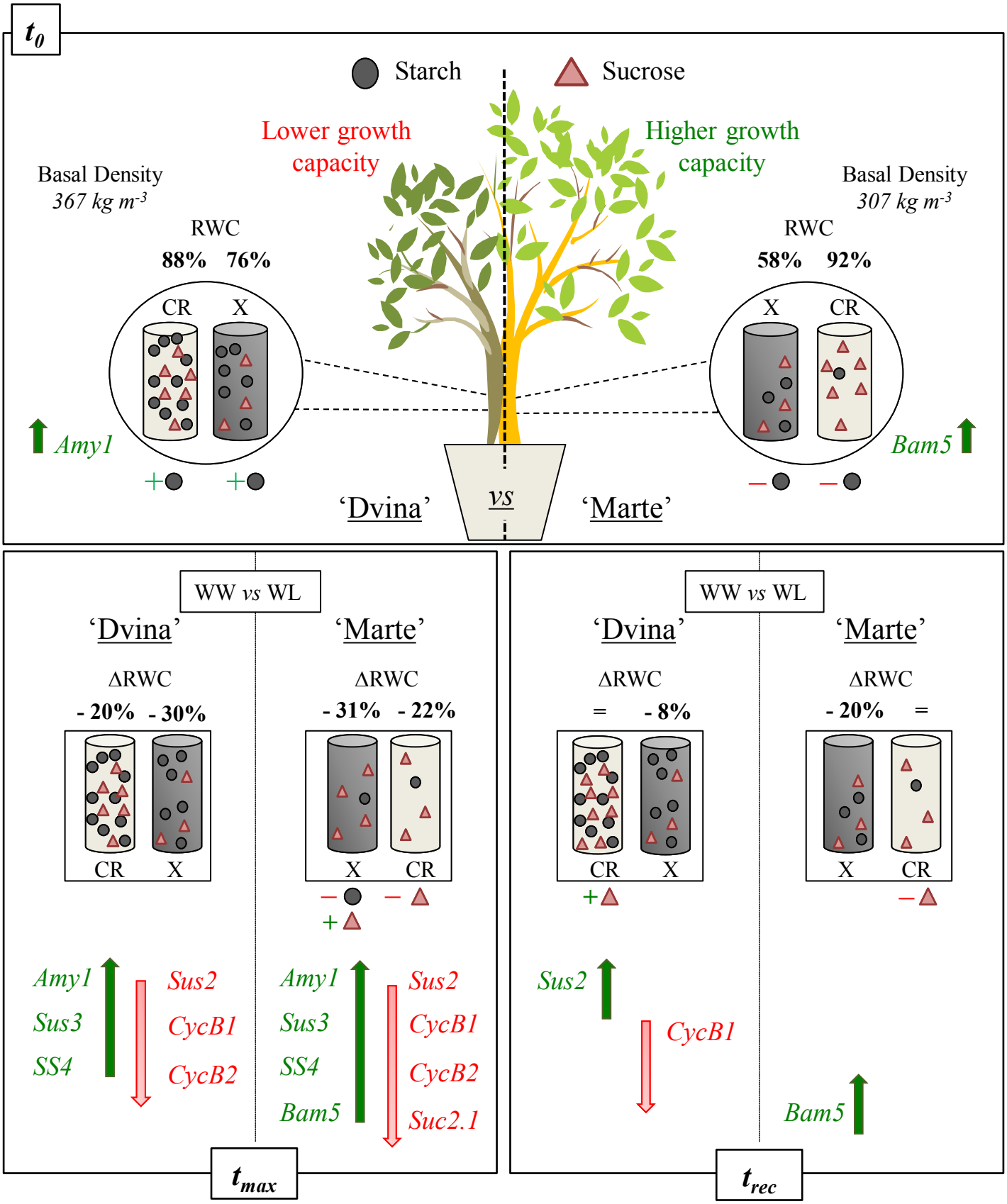
t_0
Starch
Sucrose
Lower growth capacity
Higher growth capacity
Basal Density
367 kg m-3
RWC
88% 76%
CR X
Amy1
+ +
Basal Density
307 kg m-3
RWC
58% 92%
X CR
Bam5
– –
'Dvina' vs 'Marte'
WW vs WL
'Dvina'
'Marte'
ΔRWC
- 20% - 30%
CR X
ΔRWC
- 31% - 22%
X CR
– – +
Amy1 Sus3 SS4
Sus2 CycB1 CycB2
Amy1 Sus3 SS4 Bam5
Sus2 CycB1 CycB2 Suc2.1
t_{max}
WW vs WL
'Dvina'
'Marte'
ΔRWC
= - 8%
CR X
+
ΔRWC
- 20% =
X CR
–
Sus2
CycB1
Bam5
t_{rec}